RSC Advances

PAPER

View Article Online
View Journal | View Issue

Cite this: *RSC Adv.*, 2023, **13**, 33459

Complexation study of a 1,3-phenylene-bridged cyclic hexa-naphthalene with fullerenes C_{60} and C_{70} in solution and 1D-alignment of fullerenes in the crystals†

Peifeng Mei, ‡[a] Hirofumi Morimoto,[a] Yuta Okada,[a] Kyohei Matsuo, §[a] Hironobu Hayashi, ¶[a] Akinori Saeki, [b] Hiroko Yamada §*[a] and Naoki Aratani *[a]

Received 25th September 2023
Accepted 7th November 2023

DOI: 10.1039/d3ra06526j

rsc.li/rsc-advances

To investigate the host ability of a simple macrocycle, 1,3-phenylene-bridged naphthalene hexamer **N6**, we evaluated the complexation of **N6** with fullerenes in toluene and in the crystals. The complexes in the solid-state demonstrate the one-dimensional alignment of fullerenes. The single-crystals of the C_{60}@**N6** composite have semiconductive properties revealed by photoconductivity measurements.

Introduction

Macrocyclic arenes constitute an important class of shape-persistent host molecules.[1] This system features structural rigidness, interesting optoelectronic properties, self-assembling behavior, and host–guest chemistry.[2] In many cases, they form a large cavity inside to be used for fullerene recognition.[3,4] Naphthalene is one of the simplest polycyclic aromatic hydrocarbons (PAHs) with a rigid π-plane, which has been incorporated into cycloarylenes.[5–9] We reported a macrocyclic arene, 1,3-phenylene-bridged cyclic naphthalene hexamer **N6**, that could be synthesized by a straightforward one-pot Suzuki–Miyaura reaction (Fig. 1).[10] The crystal structure showed that the **N6** had a symmetric hexagonal structure and a large cavity (d = *ca.* 15 Å). This unique structural characteristic allows **N6** to bind the spherical molecule C_{60} by forming a one-dimensional (1D)-alignment in the solid-state.[10]

Here, to examine the effects of a variation in the size and shape of fullerenes,[11] we investigated the host–guest interactions between **N6** and spherical C_{60} and ellipsoidal C_{70} using ^{1}H NMR spectroscopy in solution and single-crystal X-ray diffraction analysis in the solid state. Especially, we could determine the association constants and stoichiometry of the complexation fullerene@**N6** in solutions, for the first time, based on the statistical methodology.

Results and discussion

Complexation analysis in solution

In our previous report,[10] we could not observe the formation of the complexes of **N6** with C_{60} in chloroform due to the low solubility of C_{60}. In the present study, we analyzed complexation of **N6** in toluene as a better solvent for fullerenes. Recently, it is noticed that Job's plot is inappropriate for estimating stoichiometries in the presence of more than one complex.[11] Therefore, we attempted titration experiments with three different host–guest association models; 1 : 1, 1 : 2 and 2 : 1

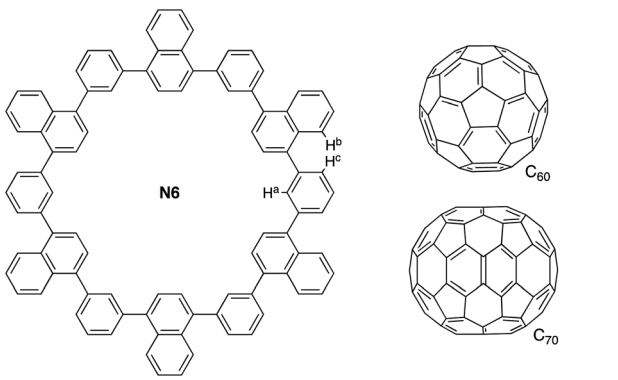

Fig. 1 Structures of a cyclic naphthalene hexamer **N6**, and fullerenes C_{60} and C_{70}.

[a]*Division of Materials Science, Nara Institute of Science and Technology (NAIST), 8916-5 Takayama-cho, Ikoma, 630-0192, Japan. E-mail: aratani@ms.naist.jp*

[b]*Department of Applied Chemistry, Graduate School of Engineering, Osaka University, 2-1 Yamadaoka, Suita, 565-0871, Japan*

† Electronic supplementary information (ESI) available: Detailed experimental procedures and additional spectroscopic data. CCDC: 2296635. For ESI and crystallographic data in CIF or other electronic format see DOI: https://doi.org/10.1039/d3ra06526j

‡ . Current address: College of Chemistry and Molecular Engineering, Peking University, Beijing 100871, People's Republic of China.

§ . Current address: Institute for Chemical Research, Kyoto University, Gokasho, Uji, Kyoto 611-0011, Japan.

¶ . Current address: Center for Basic Research on Materials, National Institute for Materials Science (NIMS), 1-2-1 Sengen, Tsukuba, Ibaraki 305-0047, Japan.

complexation.[12] Solutions of **N6** (0.4 mM) and C_{60} (0.4 mM) in toluene-d_8 were mixed in different ratios from 10 : 0 to 1 : 9 to prepare 10 samples. As an example, the chemical shift of the proton H^a in Fig. 1 was illustrated: the chemical shift originally observed at 7.64 ppm was shifted to down-field at 7.88 ppm due to the host–guest interactions (Fig. 2a). The spectral features are analogous to those of other naphthalene-C_{60} supramolecular systems.[13] This guest-binding profiles (the initial data points: 7.64, 7.53 and 7.40 ppm, 10 samples, total data points $N = 30$) were analyzed with the curve-fitting for 1 : 1, 1 : 2 and 2 : 1 binding systems (Fig. S2 and Table S1†).[12] All the fitted curves agreed with the observed chemical shift changes. It is difficult to compare the fitted curves of these models quantitatively so further analysis was made by investigation of the goodness-of-fit (GOF). To evaluate the GOF of these models, Akaike's information criterion (AIC) statistics were applied according to the recent exercise to a similar binding system.[14]

The AIC values are summarized in Table S1.† Based on the quantitative GOF analysis given by AIC calculation, the 2 : 1 additive model is the most preferred (Fig. 2b).[15] We obtained $K_{11} = 1.69\ (\pm 0.06) \times 10^4\ M^{-1}$ and $K_{21} = 4.54\ (\pm 0.42) \times 10^2\ M^{-1}$ for the first and second complexation, respectively. The smaller K_{21} value than K_{11} indicates that 1 : 1 complex is dominant in solution and 2 : 1 complex becomes coexistent when the concentration of the host is high (Fig. S3†).[15]

Previously we obtained the crystal structure of the complex of **N6** and C_{60}, which allowed us to precisely determine the 1 : 1 stoichiometry of this complex in the solid state (CCDC 1838834 for **N6**, 1838835 for C_{60}@**N6**).[10] The crystallographic analysis confirmed the π-stacking between **N6** and encapsulated C_{60}. The dihedral angles of the facing naphthalene moieties vary to maximize the interactions between the **N6** and C_{60}: upon the complexation, the dihedral angles became slightly wider from the energy minimized structure. The closest distance between the C_{60} and naphthalene is 3.32 Å in the range of π-stacking.

Then, we performed the titration between **N6** and C_{70}. The formation of the **N6**–C_{70} complex in toluene-d_8 was clearly suggested using the ^{1}H NMR (Fig. 3a). A curve-fitting simulation of guest-binding profile also supported a 2 : 1 model (Fig. S5 and Table S2†). We obtained $K_{11} = 2.52\ (\pm 0.22) \times 10^4\ M^{-1}$ and $K_{21} = 2.12\ (\pm 0.80) \times 10^2\ M^{-1}$ for the complexation (Fig. 3b). The estimated K_{11} binding constant was 1.5 times larger than that with C_{60}, inevitably due to the ellipsoidal shape of C_{70}.

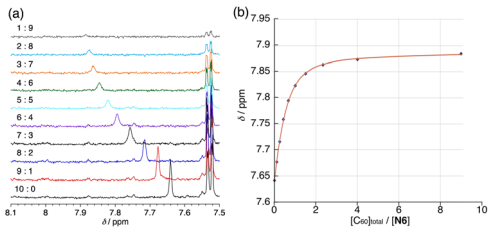

Fig. 2 (a) The chemical shift changes of inside proton resonance observed in ^{1}H NMR titration of **N6** with C_{60} in toluene-d_8. ([**N6**] : [C_{60}] = 10 : 0 to 1 : 9, the total concentration was 0.4 mM, 600 MHz, 298 K) (b) curve-fitting obtained by using the 2 : 1 binding model.

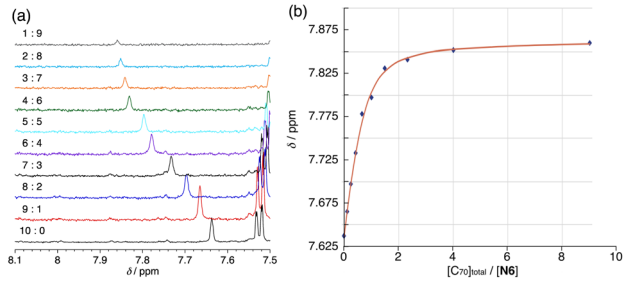

Fig. 3 (a) The chemical shift changes of inside proton resonance observed in ^{1}H NMR titration of **N6** with C_{70} in toluene-d_8. ([**N6**] : [C_{70}] = 10 : 0 to 1 : 9, the total concentration was 0.4 mM, 600 MHz, 298 K) (b) curve-fitting obtained by using the 2 : 1 binding model.

Interestingly, the peak of **N6** at 8.38 ppm assigned to H^b exhibited down-field shift upon the addition of C_{60}, while it showed up-field shift upon the addition of C_{70} (Fig. S7†). The peak at 7.53 ppm assigned to H^c similarly exhibited opposite peak shifts due to the addition of C_{60} and C_{70}. These results illustrate that the angles between naphthalene and phenylene respond to the C_{60} and C_{70} encapsulation with smaller and larger sizes, respectively.

Single-crystal X-ray analysis

Fortunately, we obtained the composite structure of **N6**–C_{70} by single-crystal X-ray diffraction analysis despite low resolution (>1.0 Å) due to very weak diffraction at the high θ angle (Fig. 4).‖ Single-crystals of **N6**–C_{70} composite were obtained by vapor diffusion of MeOH into a chlorobenzene solution. C_{70} in the crystal is nicely captured within the cavity made by **N6** with intermolecular distances in the range of 3.2–3.4 Å. Closer inspection of the crystal structure revealed that **N6** keeps a 1 : 1 complex with C_{70} similar to **N6**–C_{60} with the dihedral angles of naphthalene toward phenylene (51° and 72°). The fullerene moiety occupied at the special position refined by applying appropriate instructions. As shown in Fig. 4c, the complex also consequently forms the directly-contacting one-dimensional C_{70} array along the crystallographic *a*-axis. The long-axis of the C_{70} is tilted to the alignment direction by 33°, which is expected to increase the contact area between two fullerenes and thus to increase the interaction strengths. The closest C–C distance between fullerenes in the array is 4.1 Å, suggesting the larger electronic interaction between fullerenes than that in the **N6**–C_{60} composite (4.4 Å). In addition, the C–H···π interactions between the hydrogen atoms of the naphthalene units and the C_{70} also contribute to the stabilization of the **N6**–C_{70} assembly.

Photoconductivity measurements

The structures of **N6**–C_{60} and **N6**–C_{70} are expected to have large intermolecular orbital couplings. To discuss charge transport

‖ Crystallographic data for C_{70}@**N6**: $C_{96}H_{60}$ C_{70} C_6H_5Cl, $Mw = 2166.69$, triclinic, space group $P\bar{1}$ (#2), $a = 11.75(4)$, $b = 14.98(5)$, $c = 15.88(5)$ Å $\alpha = 106.46(3)$, $\beta = 101.62(3)$, $\gamma = 98.45(3)°$, $V = 2563(14)$ Å^3, $T = 103(2)$ K, $Z = 1$, reflections measured 5549, 4553 unique. The final R_1 was 0.1092 ($I > 2\sigma(I)$), and the final wR on F^2 was 0.4205 (all data), GOF = 1.084. CCDC: 2296635

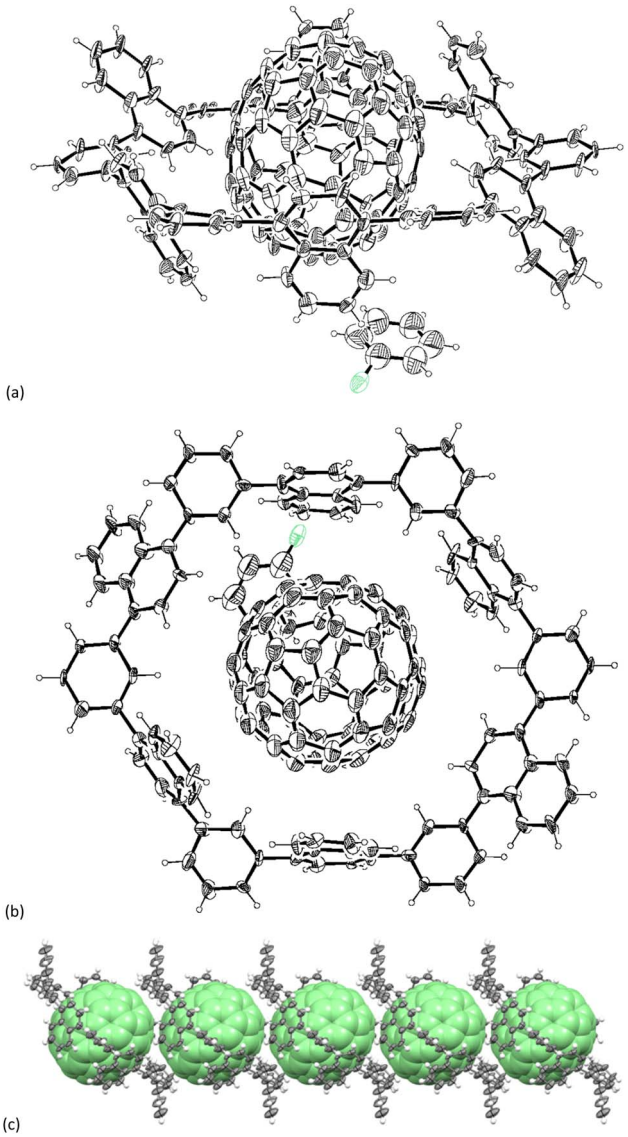

Fig. 4 X-ray structure of the **N6**–C_{70} 1 : 1 complex, ORTEP drawing from (a) the side view and (b) top view with thermal ellipsoids scaled at 25% probability. Disordered molecules are omitted for clarity. (c) A columnar array of **N6**–C_{70} along the *a*-axis. For clarity, C_{70} is shown as a space-filling model.

property in detail, the charge transfer integrals of the HOMOs (V_{hole}) and LUMOs ($V_{electron}$) between the neighbouring C_{60} and C_{70} pairs were calculated based on the crystal structures using ADF program[16] (Fig. S9†). Along the crystallographic *a*-axis, the V_{hole} and $V_{electron}$ values for C_{60} pairs were calculated to be 3.1 and 3.0 meV, respectively. On the other hand, the V_{hole} and $V_{electron}$ values for C_{70} pairs were 10.4 and 15.8 meV, respectively, higher than those of C_{60}. With these expecting charge–transport properties in mind, we conducted flash-photolysis time-resolved microwave conductivity (FP-TRMC) measurements of C_{60}@**N6**. This electrodeless method allows for evaluating short-range (~10 nm) transient conductivities of materials.[17] With a 355 nm laser pulse at 25 °C, the pseudo-conductivity ($\phi\Sigma\mu_{max}$ in $cm^2\ V^{-1}\ s^{-1}$ in which ϕ is the quantum efficiency of charge generation and $\Sigma\mu_{max}$ is the sum

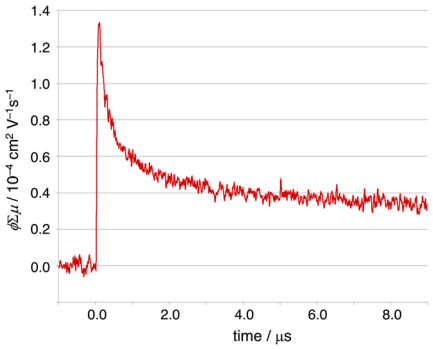

Fig. 5 FP-TRMC profile of the single-crystals (C_{60}@**N6**·PhCl) recorded at an excitation wavelength of 355 nm with a photon density of 9.1 $\times 10^{15}$ photons per cm^{-2}.

of hole and electron mobilities) of **N6**–C_{60} exhibited $\phi\Sigma\mu_{max} = 1.3 \times 10^{-4}\ cm^2\ V^{-1}\ s^{-1}$ (Fig. 5). This value is comparable to $PC_{61}BM$[18] and other conjugated molecules.[19] Unfortunately, for C_{70}@**N6** which was expected to exhibit better charge mobilities than **N6**–C_{60}, we were unable to prepare single crystals of good enough quantity to measure the FP-TRMC.

Conclusions

In summary, we present the molecular host **N6** can bind the fullerenes C_{60} and C_{70} in solution and in the solid-state. The NMR titration experiments and curve-fitting suggest that the binding profile between **N6** and fullerenes analyzed by 2 : 1 model was most likelihood with binding constants of $K_{11} = 1.69\ (\pm 0.06) \times 10^4\ M^{-1}$ and $K_{21} = 4.54\ (\pm 0.42) \times 10^2\ M^{-1}$ for C_{60}@**N6** and $K_{11} = 2.52\ (\pm 0.22) \times 10^4\ M^{-1}$ and $K_{21} = 2.12\ (\pm 0.80) \times 10^2\ M^{-1}$ for C_{70}@**N6**. In the solid-state, on the other hand, both **N6**–C_{60} and **N6**–C_{70} composites show 1 : 1 complex and make the 1D arrays of fullerenes with the aid of the **N6** agent as confirmed by the single-crystal X-ray analysis. Among these, **N6**–C_{60} exhibited the moderate $\phi\Sigma\mu_{max} = 1.3 \times 10^{-4}\ cm^2\ V^{-1}\ s^{-1}$ by FP-TRMC. We are currently investigating the host–guest chemistry of **N6** with larger fullerenes, expecting it to exhibit different selectivity and affinity.

Author contributions

The manuscript was written through contributions of all authors. All authors have given approval to the final version of the manuscript.

Conflicts of interest

There are no conflicts to declare.

Acknowledgements

This work was partly supported by Grants-in-Aid for Scientific Research (No. JP20H02816 (HH), JP20H00379 (HY), JP20H05833 (HY), JP22K19067, and JP23H01787 (NA), JP22K05255 (KM), and JP20H05836 (AS), and JST, PRESTO (No. JPMJPR21AC (HH)).

HM thanks University Fellowships for the Creation of Innovation in Science and Technology. We acknowledge Dr Mitsuaki Yamauchi (Kyoto University) for helpful discussions. This work was partially supported by ISHIZUE 2023 of Kyoto University.

Notes and references

1 S. E. Lewis, *Chem. Soc. Rev.*, 2015, **44**, 2221–2304; Y. Segawa, H. Ito and K. Itami, *Nat. Rev. Mater.*, 2016, **1**, 15002; M. A. Majewski and M. Stępień, *Angew. Chem., Int. Ed.*, 2019, **58**, 86–116.

2 K. Yazaki, L. Catti and M. Yoshizawa, *Chem. Commun.*, 2018, **54**, 3195–3206; D. Lorbach, A. Keerthi, T. M. Figueira-Duarte, M. Baumgarten, M. Wagner and K. Müllen, *Angew. Chem., Int. Ed.*, 2016, **55**, 418–421; S. Toyota and E. Tsurumaki, *Chem.–Eur. J.*, 2019, **25**, 6878–6890; M. Iyoda and H. Shimizu, *Chem. Soc. Rev.*, 2015, **44**, 6411–6424; X. Lu, S. Lee, Y. Hong, H. Phan, T. Y. Gopalakrishna, T. S. Herng, T. Tanaka, M. E. Sandoval-Salinas, W. Zeng, J. Ding, D. Casanova, A. Osuka, D. Kim and J. Wu, *J. Am. Chem. Soc.*, 2017, **139**, 13173–13183; Y. Yamamoto, K. Wakamatsu, T. Iwanaga, H. Sato and S. Toyota, *Chem.–Asian J.*, 2016, **11**, 1370–1375.

3 D. Canevet, E. M. Pérez and N. Martín, *Angew. Chem., Int. Ed.*, 2011, **50**, 9248–9259; Y. Yamamoto, E. Tsurumaki, K. Wakamatsu and S. Toyota, *Angew. Chem., Int. Ed.*, 2018, **57**, 8199–8202; H. Chen, Z. Xia and Q. Miao, *Chem. Sci.*, 2022, **13**, 2280–2285.

4 T. Iwamoto, Y. Watanabe, T. Sadahiro, T. Haino and S. Yamago, *Angew. Chem., Int. Ed.*, 2011, **50**, 8342–8344; H. Ueno, T. Nishihara, Y. Segawa and K. Itami, *Angew. Chem., Int. Ed.*, 2015, **54**, 3707–3711.

5 V. Hensel, K. Lützow, J. Jakob, K. Gessler, W. Saenger and A. D. Schlüter, *Angew. Chem., Int. Ed. Engl.*, 1997, **36**, 2654–2656; V. Hensel and A. D. Schlüter, *Chem.–Eur. J.*, 1999, **5**, 421–429.

6 Z. Sun, P. Sarkar, T. Suenaga, S. Sato and H. Isobe, *Angew. Chem., Int. Ed.*, 2015, **127**, 12991–12995; S. E. Lewis, *Chem. Soc. Rev.*, 2015, **44**, 2221–2304.

7 H. A. Staab and F. Binnig, *Tetrahedron Lett.*, 1964, **5**, 319–321.

8 J. Y. Xue, K. Ikemoto, N. Takahashi, T. Izumi, H. Taka, H. Kita, S. Sato and H. Isobe, *J. Org. Chem.*, 2014, **79**, 9735–9739 and the references are therein.

9 H.-W. Jiang, S. Ham, N. Aratani, D. Kim and A. Osuka, *Chem.–Eur. J.*, 2013, **19**, 13328–13336; Y. Nakamura, N. Aratani and A. Osuka, *Chem. Soc. Rev.*, 2007, **36**, 831–845.

10 P. Mei, A. Matsumoto, H. Hayashi, M. Suzuki, N. Aratani and H. Yamada, *RSC Adv.*, 2018, **8**, 20872–20876.

11 P. Thordarson, *Chem. Soc. Rev.*, 2011, **40**, 1305–1323; D. B. Hibbert and P. Thordarson, *Chem. Commun.*, 2016, **52**, 12792; F. Ulatowski, K. Dabrowa, T. Bałakier and J. Jurczak, *J. Org. Chem.*, 2016, **81**, 1746.

12 *Bindfit*, **http://supramolecular.org**.

13 S. Mizyed, M. Ashram, D. O. Miller and P. E. Georghiou, *J. Chem. Soc., Perkin Trans. 2*, 2001, **10**, 1916–1919; X.-W. Chen, K.-Sh. Chu, R.-J. Wei, Z.-L. Qiu, C. Tang and Y.-Z. Tan, *Chem. Sci.*, 2022, **13**, 1636–1640.

14 K. Ikemoto, K. Takahashi, T. Ozawa and H. Isobe, *Angew. Chem., Int. Ed.*, 2023, **62**, e202219059.

15 Even for a simple cycloparaphenylene (CPP) macrocycle, 1:1 and 2:1 complexes of [10]CPP and C60/C70 were detected in solution. M. Freiberger, M. B. Minameyer, I. Solymosi, S. Frühwald, M. Krug, Y. Xu, A. Hirsch, T. Clark, D. M. Guldi, M. von Delius, K. Amsharov, A. Görling, M. E. Pérez-Ojeda and T. Drewello, *Chem.–Eur. J.*, 2023, **29**, e202203734.

16 *ADF2021, Scientific Computing & Modeling (SCM), Theoreti-cal Chemistry*, Vrije Universiteit, Amsterdam, The Nether-lands, **http://www.scm.com**.

17 A. Saeki, Y. Koizumi, T. Aida and S. Seki, *Acc. Chem. Res.*, 2012, **45**, 1193–1202.

18 A. Baumann, T. J. Savenije, D. H. K. Murthy, M. Heeney, V. Dyakonov and C. Deibel, *Adv. Funct. Mater.*, 2011, **21**, 1687–1692.

19 H. Yokoi, Y. Hiraoka, S. Hiroto, D. Sakamaki, S. Seki and H. Shinokubo, *Nat. Commun.*, 2015, **6**, 8215; T. Okamoto, K. Nakahara, A. Saeki, S. Seki, J. H. Oh, H. B. Akkerman, Z. Bao and Y. Matsuo, *Chem. Mater.*, 2011, **23**, 1646–1649; J. Terao, Y. Tanaka, S. Tsuda, N. Kambe, M. Taniguchi, T. Kawai, A. Saeki and S. Seki, *J. Am. Chem. Soc.*, 2009, **131**, 18046–18047.